

# Amorphous and nanocrystalline Mg<sub>2</sub>Si thin-film electrodes

Seung-Wan Song<sup>a</sup>, Kathryn A. Striebel<sup>a,\*</sup>, Xiangyun Song<sup>a</sup>, Elton J. Cairns<sup>a,b</sup>

<sup>a</sup>*Environmental Energy Technologies Division, Ernest Orlando Lawrence Berkeley National Laboratory, Berkeley, CA 94720, USA*

<sup>b</sup>*Department of Chemical Engineering, University of California at Berkeley, Berkeley, CA 94720, USA*

## Abstract

Mg<sub>2</sub>Si films, prepared by pulsed laser deposition (PLD), were amorphous, as prepared, and nanocrystalline following annealing. Their micro-structure and electrochemical characteristics were studied by high-resolution transmission electron microscopy (HRTEM) and electrochemical cycling against lithium. HRTEM analysis revealed that some excess Si was present in the films. The more amorphous thinner film exhibited excellent cyclability. However, when the film becomes crystalline, the irreversible capacity loss was more significant during the initial cycling and after ~50 cycles. Interpretations of the superior stability of the amorphous films are examined.

Published by Elsevier Science B.V.

*Keywords:* Nanocrystalline; Thin-film electrodes; Pulsed laser deposition

## 1. Introduction

Magnesium silicide, Mg<sub>2</sub>Si, has been of interest for use as one of the alternative anode materials in rechargeable lithium batteries, but porous electrodes from the alloyed powders have shown rapid capacity decline over the first 10 cycles [1–3]. This is due to large volume and particle morphology changes that occur during lithiation and delithiation. Also it is partly due to a relatively low conductivity, such that the electrode performance depends on particle size, morphology and current density. Many studies have been performed to elucidate the capacity failure of the powder electrodes. However, the complications from amorphous carbon, binders, and electrode-electrolyte interfacial resistance inhibit precise electrochemical studies. Pure thin-film electrodes can give clearer results, yielding more information on the intrinsic properties of the intermetallics [4].

We have prepared Mg<sub>2</sub>Si thin-film electrodes on a nanometer scale by pulsed laser deposition (PLD) and some films showed excellent cyclability to 200 cycles [5]. Our previous studies of the films have shown a strong dependence of the electrochemical properties on the film crystallinity and thickness, providing insight into the capacity failure mechanism of powder electrodes. Examination of the film micro-structure using transmission electron microscopy should be more helpful than X-ray diffraction. In the present work, we describe the structural and electrochemical

characterization of two different thin Mg<sub>2</sub>Si films in the amorphous and nanocrystalline state.

## 2. Experimental

The Mg<sub>2</sub>Si films were prepared on stainless steel substrates with PLD at 250 °C for 10 and 60 min [5]. The film thickness, determined using scanning electron microscopy, was 30–380 nm depending on deposition time. The 30 nm thick film was amorphous to X-ray diffraction, whereas the 380 nm thick film was poorly crystalline. As the XRD peaks of the 380 nm film were quite small in intensity and diffuse in shape, it was annealed at 500 °C for 5 h under inert atmosphere for better micro-structural identification and was subjected to high-resolution transmission electron microscopy (HRTEM) examination using a Topcon-OO2B microscope operated at 200 kV. The annealed sample was scraped from the stainless steel substrate using a diamond pencil and the powders were dispersed in a holey carbon film with acetone in the glove box. The 30 nm film was directly deposited on a holey carbon specimen by PLD. Films as prepared were cycled at 0.1–1.0 V versus Li/Li<sup>+</sup> with 1 M LiPF<sub>6</sub>/EC + DMC(1:1) electrolyte and lithium foil counter and reference electrodes at a current density of ±35 μA/cm<sup>2</sup> using an Arbin Battery Cycler (College Station, TX) [4,5]. A porous powder film on stainless steel was prepared from a slurry of 85 wt.% Mg<sub>2</sub>Si powder, 10 wt.% carbon and 5 wt.% PVDF in NMP solution followed by ambient temperature drying in the glove box.

\* Corresponding author. Tel.: +1-510-486-4385; fax: +1-510-486-7303.  
E-mail address: [kastriebel@lbl.gov](mailto:kastriebel@lbl.gov) (K.A. Striebel).

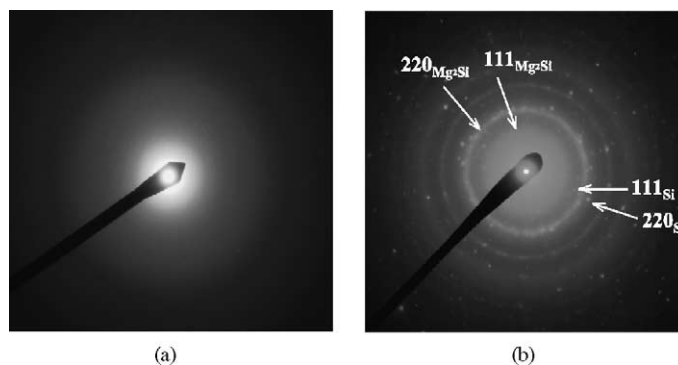


Fig. 1. Selected area electron diffraction (SAED) patterns of the (a) amorphous and (b) annealed nanocrystalline  $\text{Mg}_2\text{Si}$  films.

### 3. Results and discussion

The film as prepared with the 30 nm thickness was determined to be amorphous by HRTEM. The dispersed and very ambiguous selected area electron diffraction (SAED) pattern in Fig. 1(a) indicates its amorphous state. The SAED pattern in Fig. 1(b) of the annealed film shows a spotty ring pattern that is typical of polycrystalline material. In that pattern, the first and second order rings correspond to the (1 1 1) and (2 2 0) lattice planes with the spacings of 3.6 and 2.3 Å, respectively. The other rings are unclear, attributed to imperfect crystalline characteristics of this film. The presence of Si phase in the material was identified by SAED pattern indexing (Fig. 1(b)). A few spots of Si are observed near the strong rings of  $\text{Mg}_2\text{Si}$ . Actually polycrystalline silicon has a similar crystal structure and SAED pattern with interplane spacings of 3.1 and 1.9 Å corresponding to (1 1 1) and (2 2 0) lattice planes [6]. According to the Mg–Si phase diagram, the  $\text{Mg}_2\text{Si}$  phase is stable up to  $>1000^\circ\text{C}$  [7]. In this context, annealing of the film at  $500^\circ\text{C}$  might not cause the phase change. It is thus obvious that the isolated Si is not caused by segregation from  $\text{Mg}_2\text{Si}$  during annealing but was already present in the film as prepared, and was undetectable by XRD. The annealing promoted crystal

growth of Si as well as  $\text{Mg}_2\text{Si}$ . The Si in the amorphous film also should be amorphous.

The lattice image (Fig. 2) of the annealed film exhibits polycrystalline particles with a few tens of nanometer in size, but those particles aggregated to form larger ones. The regularly spaced array of planes in the enlarged image is of the cubic ( $Fm\bar{3}m$ )  $\text{Mg}_2\text{Si}$ . The lattice fringes spaced by 2.3 and 3.6 Å, correspond to the  $\text{Mg}_2\text{Si}$  (2 2 0) and (1 1 1) planes, respectively, are dominant over all the regions of the particle. This  $\text{Mg}_2\text{Si}$  film is nanocrystalline. The ambiguous features of crystal edges and small particle size should allow facile lithium diffusion.

Fig. 3 shows differential capacity plots for the 5th and 200th cycles for the amorphous (30 nm thick) and nanocrystalline films (380 nm thick) as prepared. Both films show significant lithium insertion to the  $\text{Mg}_2\text{Si}$  matrix at potentials around 0.2 V, consistent with the results of other reports [1–3]. It was reported that the  $\text{Li}_2\text{MgSi}$  ternary phase forms accompanied by formation of Li–Mg alloy at 0.1 V and Li–Si alloy at about 0.4 V during lithium insertion into the  $\text{Mg}_2\text{Si}$  [2,3]. The  $\text{Li}_2\text{MgSi}$  converts to  $\text{Mg}_2\text{Si}$  upon lithium discharge and the alloys also discharge lithium exhibiting peaks at 0.26 and 0.6 V, as seen in Fig. 3. The cyclability of the amorphous film was excellent up to 200

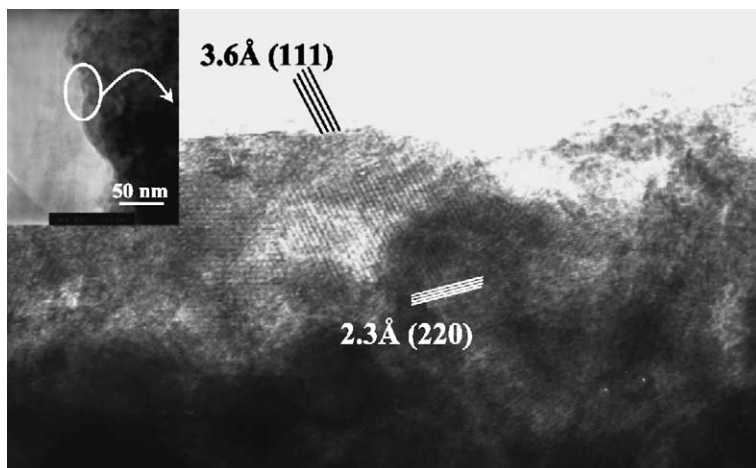


Fig. 2. Lattice image of the annealed nanocrystalline  $\text{Mg}_2\text{Si}$  film.

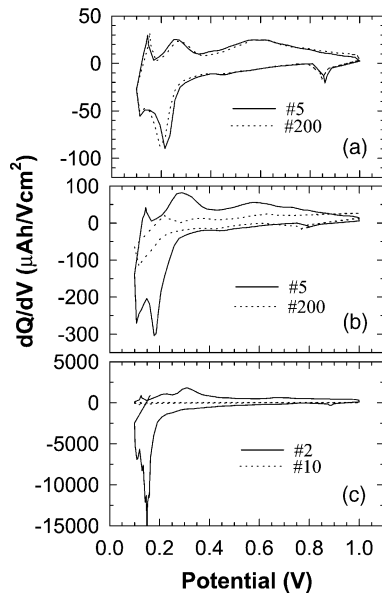


Fig. 3. Differential capacity plots of the (a) amorphous (30 nm thick), (b) nanocrystalline (380 nm thick) as prepared, and (c) porous powder film of  $\text{Mg}_2\text{Si}$  at different cycle numbers.

cycles and a stable capacity (Fig. 3(a)) greater than 2200 mAh/g, whereas the nanocrystalline film showed a stabilized initial capacity of 790 mAh/g followed by slow capacity fade after 50 cycles (Fig. 3(b)). The thicker film was more crystalline and showed worse cycling behavior than the thinner film. Amorphous films should have less structural or mechanical strain caused by lattice volume change than crystalline films, during the reaction with lithium. For highly crystalline particles, as for the porous film shown in Fig. 3(c), severe capacity fade occurred. Self-discharge reaction was certainly observed in the films, reflecting side reaction with the electrolyte forming a SEI layer [5]. The SEI layer usually forms during the initial cycle. Much of the 30 nm thick amorphous film may be utilized for the SEI layer preventing further growth of surface layer by the electrode–electrolyte reaction during cycling, resulting in stable cyclability. The excess amorphous Si can be partly responsible for the high capacity and cyclability of the thin amorphous film. The nanocrystalline film undergoes large

volume change causing structural–mechanical disintegration of the film and weakening of film–substrate adherence during cycling.

#### 4. Conclusion

Film structure was identified as cubic  $\text{Mg}_2\text{Si}$  by HRTEM. The 30 nm thick film was totally amorphous but showed superior cyclability over 200 cycles in contrast to the nanocrystalline film, which lost capacity in 50 cycles. Shorter PLD time significantly modified the film structural properties, which is closely related to the enhancement of capacity and cyclability. It is interpreted that the crystalline characteristics of the film is one of the causes for capacity fade during cycling, as observed in porous intermetallics powder electrodes.

#### Acknowledgements

This work was supported by the Office of Energy Research, Basic Energy Sciences, Chemical Sciences Division of the Department of Energy under contract no. DE-ACO3-76SF00098. We are grateful to Ronald P. Reade for the film preparation with PLD, and Gregory A. Roberts for the target and helpful discussion.

#### References

- [1] H. Kim, J. Choi, H.J. Sohn, T. Kang, J. Electrochem. Soc. 146 (1999) 4401.
- [2] T. Moriga, K. Watanabe, D. Tsuji, S. Massaki, I. Nakabayashi, J. Solid State Chem. 153 (2000) 386.
- [3] G.A. Roberts, E.J. Cairns, J.A. Reimer, J. Power Sources 4819 (2002) 1.
- [4] K.A. Striebel, A. Rougier, C.R. Horne, R.P. Reade, E.J. Cairns, J. Electrochem. Soc. 146 (1999) 4339.
- [5] S.W. Song, K.A. Striebel, R.P. Reade, G.A. Roberts, E.J. Cairns, J. Electrochem. Soc. 150 (2003) A121.
- [6] D.P. Yu, C.S. Lee, I. Bello, X.S. Sun, Y.H. Tang, G.W. Zhou, Z.G. Bai, Z. Zhang, S.Q. Feng, Solid State Commun. 105 (1998) 403.
- [7] A. Nayeb-Hashemi, J. Clark, Phase Diagrams of Binary Magnesium Alloys, ASM International, 1988.